2024 IEEE/ASME International Conference on Advanced Intelligent Mechatronics (AIM)
July 15-19, 2024. Boston, MA, USA

Power-assist Control of an Add-on Type Electric Wheelchair with the Active-caster

Keiichi Hongo and Masayoshi Wada

Abstract— **In this paper, we propose an add-on electric drive system for manual wheelchairs using one active caster, which has been the driving wheel developed for omnidirectional robots. Active casters can instantly generate a velocity vector in any direction by the cooperative control of two motors. The active-caster is installed at the rear of a manual wheelchair to control the two degrees of freedom of the wheelchair movements: forward movement and turning. Furthermore, a torque detection system is installed into the power transmission of the active caster to measure the direction and magnitude of an applied force acting on the wheel. A power assist control of the wheelchair is performed based on this force detection. Therefore, there is no need to install any force detection devices on a manual wheelchair, it is possible to create wheelchair motions with electric motor support by applying force to any part of the wheelchair. This makes it possible for the wheelchair to be moved by pushing and pulling the wheelchair by a caregiver, by operating the large wheels by the passenger himself, by pushing the floor with his legs, or by pushing and pulling the desk with his hands. We demonstrate the feasibility of these functions through experiments using a prototype wheelchair.**

I. Introduction

In Japan, the declining of birth rates and working-age population is decreasing year after year [1][2]. Therefore, research and development of human support devices have become even more important. Against this background, research on intelligent control of wheelchairs is being actively conducted[3][4][5]. The author's group is conducting research on an electric mobile system that can be attached to lightweight and compact manual wheelchairs. In the proposed system, a single active-caster with a force sensing function is attached to the rear of a manual wheelchair, and the motion of the wheelchair is controlled by utilizing electric power provided by the active-caster. In this paper, we report on an electric wheelchair that is equipped with a force detection device on active-casters and operates with the assistance of an electric device using external force without the need to attach a force sensor to a manual wheelchair.

II. Existing Technologies

A lot of research and development has been conducted in the past to support wheelchair motions by the power of electric motors. For this purpose, a device similar to the throttle handle used on motorcycles is installed at the back position of the wheelchair seat for the caregiver to operate [6][7][8]. In addition, an assist system for users is developed in which round ringbars with torque sensors are equipped on the large wheels of a wheelchair that the wheelchair user can operate, and electric motors assist the rotations of the large wheels based on the detected torque information, which enables a wheelchair to operate with small forces in the same manner as a normal manual wheelchair[9]. These systems can work when an operational force is applied on a specific point of a wheelchair, such as a throttle handle or a force-sensing mechanism. Therefore, the assisted operation methods are limited.

On the other hand, an assist system with a fixed single drive-wheel was proposed in which external forces are estimated by a disturbance observer of the electric motor and an assistance torque are provided only in the wheel rolling direction [10][11]. However, this can only support driving in the back-and-forth direction of the wheelchair and turning motion cannot be supported.

III. Differential Drive Active Caster

Figure 1 shows a top view of the active caster[12]. The configuration of the active caster is the same as a passive caster which has an offset distance between the wheel axle and the steering shaft and the wheel steers eccentrically.

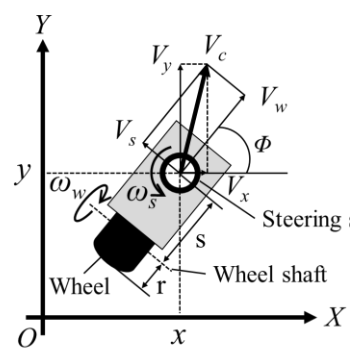

Fig.1 Velocity vector generated by active-caster

The active-caster system generates a velocity vector on the position of the center steering shaft in any direction. Equation (1) represents a kinematics of the active-caster. The velocity component V_w in the wheel-rolling direction is generated by the rotation of the wheel axle ω_w while the velocity component in the lateral direction of the wheel V_s can be provided by the rotation of the steering shaft ω_s. Therefore, independent speed control of the wheel rotation and the steering rotation enables

Keiichi Hongo is a graduate student in the Department of Electrical Engineering, Tokyo University of Science, 6-3-1 Niijyuku, Katsushika-ku, Tokyo 125-8585, Japan, (e-mail: 4323539@ed.tus.ac.jp)

Masayoshi Wada is with the Department of Electrical Engineering, Tokyo University of Science, 6-3-1 Niijyuku, Katsushika-ku, Tokyo 125-8585, Japan, (e-mail: m-wada@rs.tus.ac.jp)

the steering center to move in vector V_c in Fig.1, namely in any direction with any magnitude.

$$\begin{bmatrix} V_x \\ V_y \end{bmatrix} = \begin{bmatrix} r\cos\phi & -s\sin\phi \\ r\sin\phi & s\cos\phi \end{bmatrix} \begin{bmatrix} \omega_w \\ \omega_s \end{bmatrix} \quad (1)$$

Where r is a radius of the wheel, s is a caster offset and ϕ is a wheel orientation relative to the mobile base.

In the conventional designs, a steered wheel was designed to rotate a wheel by one motor while a steering shaft was driven by another motor. By this design, the motor for the steering shaft would almost stop when traveling in a certain direction. This reduces the operating efficiency of the motors. To solve this problem and create a compact and lightweight electric unit, we propose the differential type wheel mechanism to drive the active-caster. Figure 2(a) shows schematics of the differential drive type active-caster[13]. Two motors are fixed on the mounting base, and a power of the motor1 is transmitted through spar gears and bevel gears to a left side of a tire as shown in the figure. A power of motor2 is transmitted in the same manner as the motor1 but the torque is applied to the right side of the tire. With this structure, if the motors are driven to rotate in the same direction at the same speed, only the wheel axle will rotate, and if the motors are driven to rotate in opposite directions at the same speed, only the steering shaft will rotate. In this way, the average of the rotation speeds of the two motors is the wheel rotation speed, and the difference is the steering shaft rotation speed. The relationships between the motor rotation and wheel and steering rotations are represented as eq.(2). The inverse equation of eq.(2) is represented as eq.(3). The kinematics of the differential type active-caster can be derived by eq.(1) and eq.(3).

Therefore, even when a wheelchair is traveling with the wheels facing in a certain direction, the wheels are rotated by the two motors. This feature contributes to improve the drive efficiency of the motors.

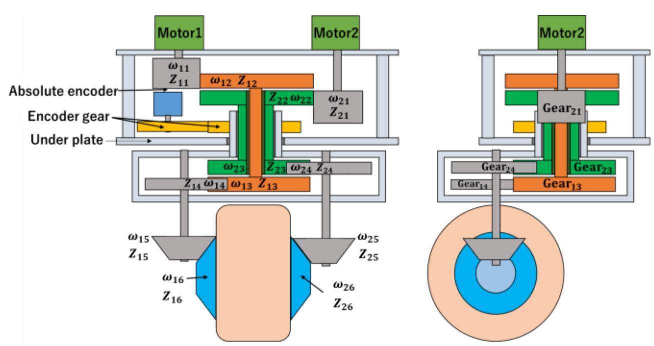

(a) Front view (b) Side view

Fig.2 Differential drive type active-caster design

$$\begin{bmatrix} \omega_1 \\ \omega_2 \end{bmatrix} = \begin{bmatrix} G_{11} & -G_{12} \\ -G_{21} & -G_{22} \end{bmatrix} \begin{bmatrix} \omega_w \\ \omega_s \end{bmatrix} \quad (2)$$

$$\begin{bmatrix} \omega_w \\ \omega_s \end{bmatrix} = \frac{1}{G_{21}G_{12} + G_{11}G_{22}} \begin{bmatrix} G_{22} & -G_{12} \\ -G_{21} & -G_{11} \end{bmatrix} \begin{bmatrix} \omega_1 \\ \omega_2 \end{bmatrix} \quad (3)$$

Where G_{ij} is a gear ratio like $G_{i1} = \frac{Z_{i2}Z_{i4}Z_{i6}}{Z_{i1}Z_{i3}Z_{i5}}$ and $G_{i2} = \frac{Z_{i2}}{Z_{i1}}$ $(i = 1,2)$ and Z_{ij} $(j = 1\text{-}6)$ is a number of teeth.

IV. Force Sensing System

A force sensing system is installed on the differential drive type active caster mentioned in the previous section. A conceptual diagram is shown in Fig.3. The first reduction gears on the motor shafts shown in Fig.2 are replaced by belt-pully transmissions. The rotation of the motor is transmitted to the large pulley via the toothed belt. For measuring the tension of the transmission belt between the small pulley on the motor shaft and the large pulley, idle rollers supported by beams with strain gauges are loaded to the belt as shown in Fig.3. Two strain gages are attached on both side of one beam, and one bridge circuit is assigned to a strain gauge pair to obtain one analog output from each beam. The bridge circuit is Two-gauge method which uses two variable resistors and two constant resistors shown in Fig.3. These variable resistors are attached on both sides of one beam. The operating force creates the imbalance of the tensions of two belts because reduction ratio is large and change value of variable resistors. When the tension of the belt varies, the bridge circuit provides an analog voltage proportional to the tension change. There are eight strain gauges in total for the active-caster, by that 4 channels of analog output are obtained to measure two torques on the transmissions by two drive motors.

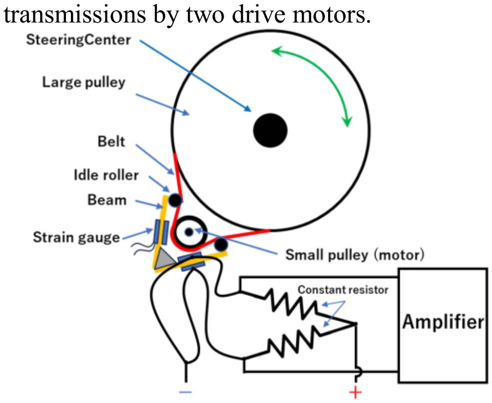

Fig.3 Force sensing system

Since Fig.3 shows the force sensing system for 1axis, we need to prepare two force sensing systems to realize the force detection in all directions in the horizontal plane.

We can derive relationship between detected torque information and external force by using kinematics of the differential drive type active-caster. The inverse kinematics of eq.(1) and gearing equation eq.(3), we derive following relationships between motor rotations and generated velocity components.

$$\begin{bmatrix} \omega_1 \\ \omega_2 \end{bmatrix} = \begin{bmatrix} G_{11} & -G_{12} \\ -G_{21} & -G_{22} \end{bmatrix} \begin{bmatrix} \frac{1}{r}\cos\phi & -\frac{1}{r}\sin\phi \\ \frac{1}{s}\sin\phi & \frac{1}{s}\cos\phi \end{bmatrix} \begin{bmatrix} V_x \\ V_y \end{bmatrix} \quad (4)$$

By the principle of virtual work to the eq.(4), a following equation can be derived which represents a relationship between detected external torques and an applied force to the active-caster mechanism.

$$\begin{bmatrix} F_x \\ F_y \end{bmatrix} = \begin{bmatrix} \frac{1}{s}\cos\phi & -\frac{1}{r}\sin\phi \\ \frac{1}{s}\sin\phi & \frac{1}{r}\cos\phi \end{bmatrix} \begin{bmatrix} -G_{22} & -G_{12} \\ -G_{21} & G_{11} \end{bmatrix} \begin{bmatrix} \tau_1 \\ \tau_2 \end{bmatrix} \quad (5)$$

Where $[F_x, F_y]$ is a force vector generated or applied at the center of the steering axis of the active-caster, and $[\tau_1,\tau_2]$ is a torque vector measured by the proposed force sensing system.

V. POWER-ASSIST WITH ADMITTANCE CONTROL

The admittance control is applied to achieve stable wheelchair power assist operation because it can simulate various dynamic characters by changing admittance parameter. Also, the system stabilizes because the motor controllers control speed-based control. Using the force information measured by the active caster force sensing system, the virtual motion model defined in the controller calculates wheelchair a behavior and drives the active casters to achieve that behavior by sending speed commands to the two motors. The component of the detected force along X-axis creates the back-and-forth motion of the wheelchair, and the lateral component along Y-axis generates the turn motion of the wheelchair. Note that the lateral force component is converted into a moment that causes the wheelchair to turn depending on the distance from the center of the wheelchair to the position where the active-caster is attached.

Equation 6 shows the virtual model used for admittance control. The mass *M*, translational viscosity coefficient *C*, moment of inertia *I*, and rotational viscosity coefficient *D* are pre-defined, and the detected force $[F_x, F_y]$ is used to drive the virtual model. The behaviors in the translation *V* and rotation *Ω* calculated by the virtual model are sent to a feedback controller as velocity commands of the wheelchair.

$$\begin{bmatrix} M & 0 \\ 0 & I \end{bmatrix} \begin{bmatrix} \dot{V} \\ \dot{\Omega} \end{bmatrix} + \begin{bmatrix} C & 0 \\ 0 & D \end{bmatrix} \begin{bmatrix} V \\ \Omega \end{bmatrix} = \begin{bmatrix} F_x \\ -LF_y \end{bmatrix} \quad (6)$$

Where L is a distance from the wheelchair center to the active-caster as shown in Fig.4.

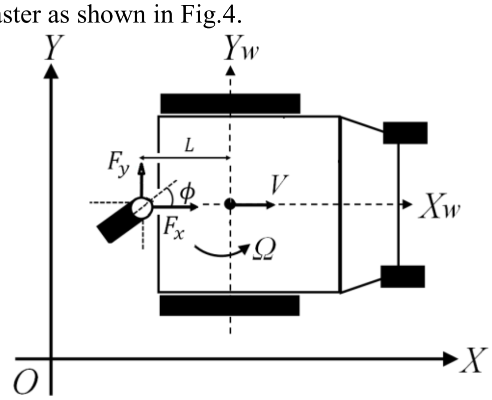

Fig.4 Detected force and motion of a wheelchair

Fig.5 shows the sub-block diagram of power-assist control and the motor unit. The force vector and steering axis angle are applied to the kinematic model to calculate the reference velocity. In this study, the reference velocity is calculated by integrating the operating force vector. Next, the difference between the calculated reference velocity and the measured motor velocity obtained from the encoder is determined. Finally, this is applied to PID control to convert it into a command current, which is then sent as a command to the motor.

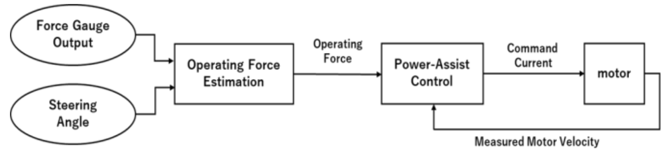

Fig.5 Block diagram of power-assist control

VI. PROTOTYPING

Figure 6(a) shows the prototype of the active caster. A traction motor is a 60W brushless DC motor integrated with a gear head with a reduction ratio of 1/41. Two motors both have the same specification are installed on the active-caster. The power of the output shaft of the motor reduction gear is transmitted to wheel mechanism by a belt-pulley(20:130) in the first reduction and then transmitted by the spur gears(1:1) in the second stage, while the final bevel gears (20:30) drive a tire . The same power trains are installed for two motors that transmit the power to either side of the wheel. The wheel radius is 59mm and the caster offset is 52mm.

For measuring the tension of the transmission belt between the output shaft of the gear head and the large pulley, an idle roller supported by a beam with strain gauges provides pre-load to the belt as shown in Fig.6(b). Two strain gauges are attached on both side of the beam, and one bridge circuit is assigned to a strain gauge pair to obtain one analog output from each beam. When the tension of the belt varies, the bridge circuit provides an analog voltage proportional to the tension change. There are eight strain gauges in total for the active-caster, by that 4 channels of analog output are obtained to measure two torques on the transmissions by two drive motors.

Figure7 shows the manual wheelchair with the prototype active caster. The diameter of the large wheel of the manual wheelchair is 508mm(20inch) and the wide of the wheelchair is 460mm. The active-caster is installed on the backside of the manual wheelchair with *L*=140mm from the midpoint of the large wheels.

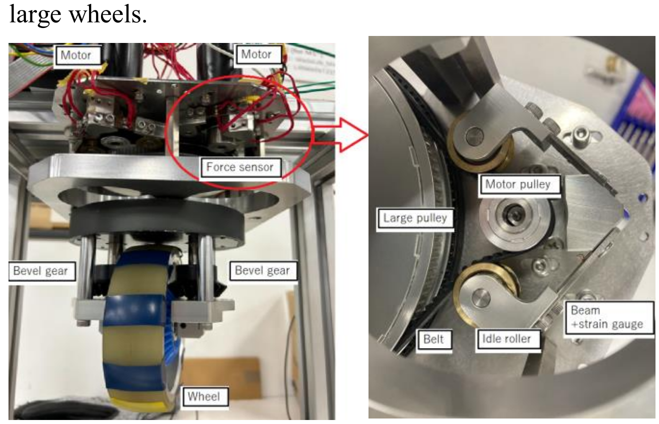

(a) Active-caster overview (b) Force senser mechanism

Fig.6 Active-caster with force sensing system

Fig.7 Overview of the prototype wheelchair

Figure8 shows an architecture of prototype wheelchair system. This system is implemented Windows11, which gets the information of the force and the motor velocity and controls two motors. The motor velocity is measured by a motor driver.

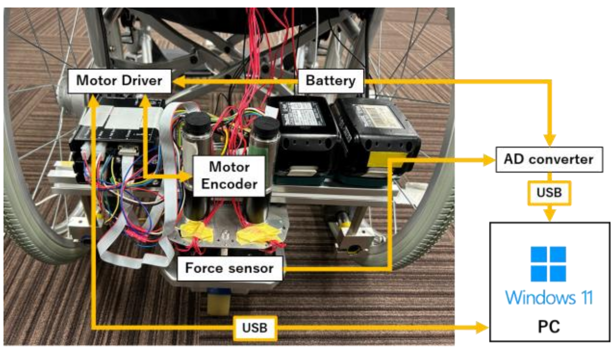

Fig.8 Architecture of prototype wheelchair system

VII. Experiments

In this section, we conducted experimental verification using the prototype wheelchair to demonstrate the ability to perform force estimation and power-assisted maneuvering. Estimated operation force outputted zero when it exceeded the threshold to reduce the affected of noise. The power-assist control cycle in Fig.5 was about 30ms. In eq.(6), the mass M was 112 kg and the moment of inertia I was 1.18×10^{-2} kg $\times$ m^2. This value was determined by prior experiments. The translational viscosity coefficient C and the rotational viscosity coefficient D was zero to make the behavior of power-assist easier to understand.

A. Power assist test operated by a care giver

We conducted operational verification using the prototype wheelchair. A user sat on the wheelchair and a care giver manually applied a force on a grip of the manual wheelchair as shown in Fig.9. Fig.10(a) shows a detected force information by the force sensing system. At approx.3second in the experiment, large forces are detected in the positive side of the X-direction (forward of the wheelchair) while small forces in positive and negative were detected along Y-axis. By the applied force, the wheelchair accelerated greatly in X-direction and keeps a certain velocity as shown in Fig.10(b). The force information drove the virtual model based on the admittance control. In this experiment, the dumping coefficient was set to vary small value then wheelchair speed was not reduced quickly. A series of snap shots of the experiment are shown in Fig.15(a)-(d).

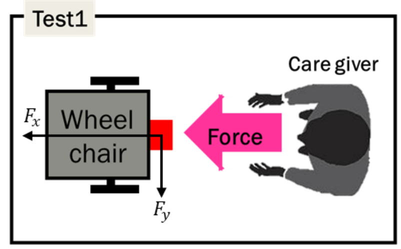

Fig.9 Power assist test operated by a care giver

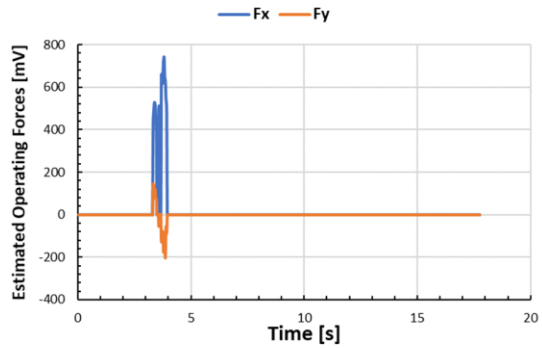

(a) Detected force applied by a care giver

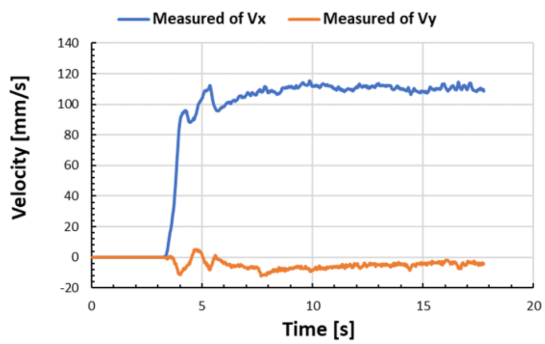

(b) Wheelchair motion operated by a care giver

Fig.10 Experimental results of the care giver operation

B. Power assist test operated by a wheelchair user 1

We verified that the power assist control is available even when a user applies a force on the wheelchair's handlebar. In this verification, a user was seated in the wheelchair, and operating forces were applied to rotate handlebars on the left and right large wheels in the same manner of the manual operation. Fig.12(a) shows a detected force information by the force sensing system. At the 3second, the positive force in X-direction was applied. By the propelling force the wheelchair started to move and maintain a certain velocity on forward direction as shown in Fig.12(b). At 11second, quite large negative force was applied to stop the wheelchair. Just right after the moments, the wheelchair started to move backward. Through this experiment, small forces are detected in Y-direction but the wheelchair did not show large movements in lateral direction. A series of snap shots of the experiment are shown in Fig.16(a)-(f).

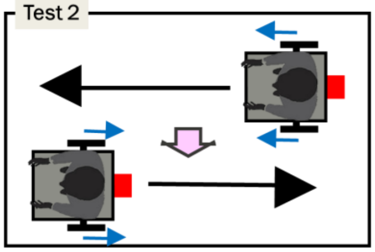

Fig.11 Power assist test operated by a user (forward-back)

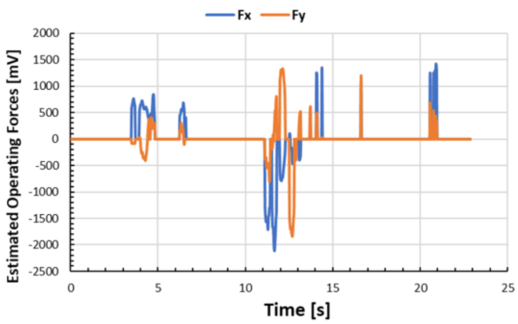

(a) Detected force applied at handle bar by a user

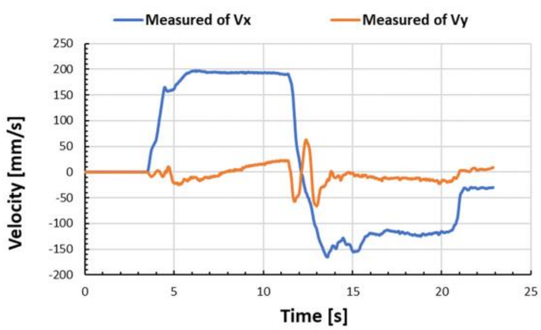

(b) Wheelchair motion operated by a user

Fig.12 X and Y Speeds forward/backward motion

C. *Power assist test operated by a wheelchair user 2*

We conducted verification of curve motion. In this experiment, the forces different in magnitude were applied to the left and right wheels for curve motion. Fig.14(a) shows detected force in the experiment. Between 3seconds to 4seconds, both force components in X and Y directions are detected simultaneously. This means that the active-caster moves inclined direction to drive the wheelchair to perform curve motion. However, the force in X and Y directions are detected at 5, 9 and 36 seconds. This is the noise by friction with the floor. In Fig.14(b), It is seen that both velocity components in X and Y directions are generated. A series of snap shots of the experiment are shown in Fig.17(a)-(d).

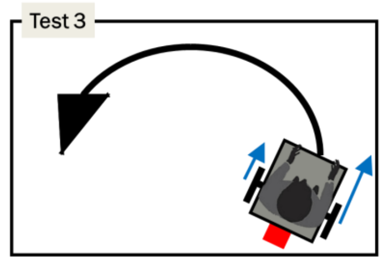

Fig.13 Power assist test operated by a user (turn)

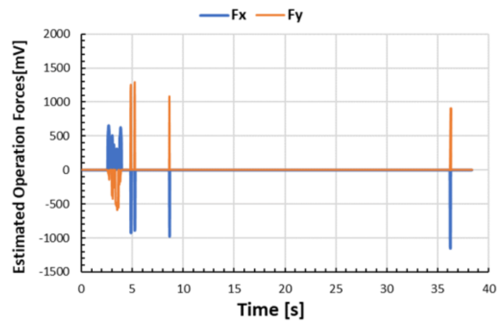

(a) Detected force applied at handle bar by a user

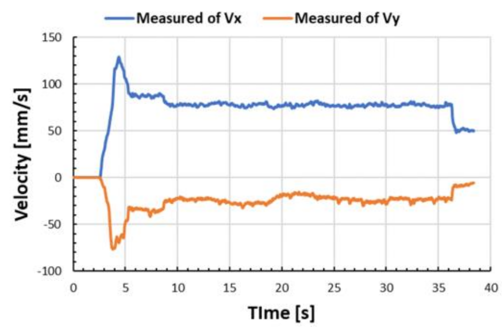

(b) Wheelchair motion operated by a user (curve)

Fig.14 X and Y Speeds in curve motion

VIII. CONCLUSION

In this paper, we proposed an active-caster electric drive system with force sensing function for power-assist control of manual wheelchairs. The operational forces were detected by measuring the tensions of transmission belts by strain gauges installed on the active-caster mechanism. The force detection performance were confirmed by a fundamental experiment in which sensitivities on the detection of applied force and moment were enough for power assist control such as for handle operations by care givers or for wheelchair operations using the hands and feet of users. To drive a manual wheelchair based on the force information, we applied the admittance control to the active-caster mechanism. Using a prototype wheelchair with the active-caster and force detection system, we conducted experiment in which the wheelchair was operated by a caregiver by applying force on a handle. Self-propelling experiments were also conducted where the wheelchair was operated by a wheelchair user by rotating the large wheels. Through these experimental results, the successful behaviors of the power-assisted manual wheelchair were achieved which demonstrated the effectiveness of the proposed system. Since the reduction gear installed on the current prototype wheelchair has high gear ratio, the velocity of the wheelchair was limited.

In the future, we will modify the design of the drive system to improve the force sensitivity and the drive speed.

ACKNOWLEDGMENT

This research was partly supported by KAKENHI, 20H04562.

REFERENCES

[1] Statistics Bureau of Japan, https://www.stat.go.jp/data/jinsui/2021np/index.html [Accessed January 17, 2024]

[2] Ministry of Health, Labour and Welfare, https://www.mhlw.go.jp/toukei/saikin/hw/jinkou/tokusyu/syussyo07/dl/01.pdf [Accessed January 17, 2024]

[3] Y.Kaida, T.Murakami, "The Electric Wheelchair Control Using Electromyography Sensor Of Arm Muscle [in Japanese]", *IEEJ Transactions on Industry Applications*, vol.126, No.2, pp.137-142, 2006

[4] H,Seki, T.Kuramoto, Proposal of Target Position Estimation Type Driving Control and Operation Training System for Power-Assisted Wheelchairs [in Japanese], *Transactions of the Institute of Systems, Control and Information Engineers*, vol.32, No.10, pp.378-387, 2019

[5] R.Hardiansyah, A. Ainurrohmah, Y. Aniroh, F.H.Tyas, "The Electric Wheelchair Control Using Electromyography Sensor Of Arm Muscle ", *2016 International Conference on Information, Communication Technology and System*, pp.129-134, 2016

[6] Ting-Shuo Chen, Chung-Hsien Kuo and Po-Chun Chia, "Development of a Wireless Sensor Node Based Pushrim Activated Wheelchair Controller", *2010 IEEE International Conference on Systems*, Man and Cybernetics, 2010.

[7] Yamaha, https://www.yamaha-motor.co.jp/wheelchair/lineup/active-plus/ [Accessed January 17, 2024]

[8] TGA Mobility Ltd., https://www.tgamobility.co.uk/product/wheelchair-powerpack-solo/[Accessed April 29, 2024]

[9] Yamaha, https://www.yamaha-motor.co.jp/wheelchair/lineup/jwx2/ [Accessed Feb. 17, 2024]

[10] P. Li, C. Liu, H. Liang, N. Ogawa, C. Zhu, "Development of Power Add-on Unit for Manual Wheelchair and Its Sensorless Power Assistance Control", *The 12th International Convention on Rehabilitation Engineering and Assistive Technology*, pp. 324-328, 2018.

[11] Permobile, Co., https://permobilkk.jp/products/smartdrive [Accessed Feb. 17, 2024]

[12] M. Wada and S. Mori, "Holonomic and Omnidirectional Vehicle with Conventional Tires," *Proceedings of the 1996 IEEE Int. Conf. on Robotics and Automation (ICRA96)*, pp. 3671–3676, 1996.

[13] Taisei Nakayama and Masayoshi Wada, "Study on an Add-on Type Electric Wheelchair Using Active Caster with the Differential Mechanism", *Journal of Robotics and Mechatronics*, vol.35, No.1, pp.

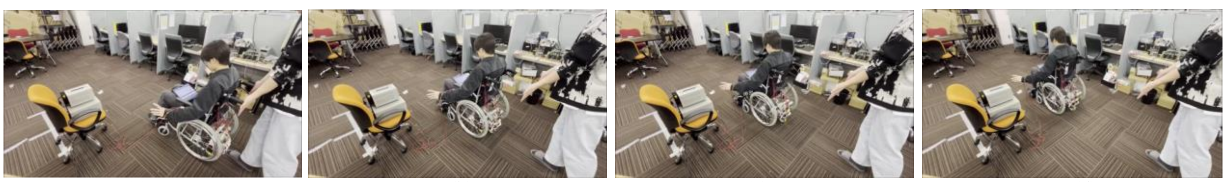

(a) (b) (c) (d)

Fig.15 Snapshots of the experiment (operated by a care giver)

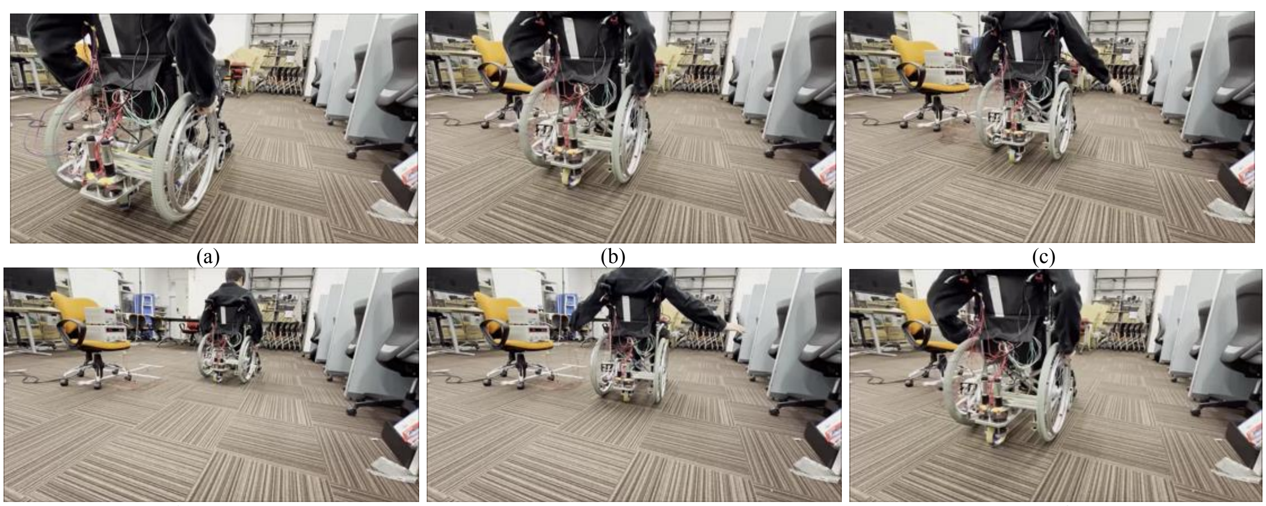

(a) (b) (c)

(d) (e) (f)

Fig.16 Snapshots of the experiment (operated by a user : going forward and back)

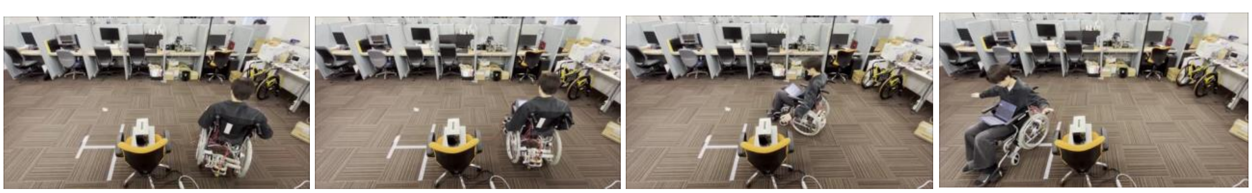

(a) (b) (c) (d)

Fig.17 Snapshots of the experiment(operated by a user : curving motion)